

Report 78-11

September 1978

COMPENSATION OF T-28 UPDRAFT MEASUREMENTS FOR  
AIRCRAFT-INDUCED EFFECTS USING ANGLE-OF-ATTACK  
DATA

By: R. Ananthakrishna Sarma

Prepared for :

Convective Storms Division  
National Center for Atmospheric Research  
P. O. Box 3000  
Boulder, CO 80307

Subcontract No. NCAR 182-71

Institute of Atmospheric Sciences  
South Dakota School of Mines and Technology  
Rapid City, South Dakota 57701

## ABSTRACT

This thesis describes a method derived analytically to compute updraft velocities in cumulus clouds from data collected by the T-28 armored aircraft operated by the Institute of Atmospheric Sciences, South Dakota School of Mines and Technology. This method is suggested as an improvement on the empirical updraft equation evolved by W. Sand in 1974. It involves the resolution of the relative wind vector into components. Using the aircraft angle of attack and attitude information, the vertical velocity of the air with respect to the aircraft is calculated. Then the updraft velocity is derived from the vertical velocity of the aircraft itself, corrected for this relative motion of the air. Corrections for aircraft induced effects such as the deflection of the angle of attack sensor vane by airflow around the wing and the vertical velocity induced by the roll motion of the aircraft are also included. An error analysis is also done on the final equation.

TABLE OF CONTENTS

	<u>Page</u>
ABSTRACT . . . . .	ii
LIST OF FIGURES . . . . .	iv
LIST OF TABLES . . . . .	v
1. INTRODUCTION . . . . .	1
1.1 Techniques for Measuring Vertical Air Motions . . . . .	1
1.2 Updraft Measurements with the Armored T-28 Aircraft (Sand's Method) . . . . .	2
1.3 Angle of Attack Method of Determining Updraft Speeds . . . . .	3
2. THE BASIC THEORY BEHIND UPDRAFT CALCULATIONS USING THE ANGLE OF ATTACK METHOD . . . . .	5
3. MEASURING THE ANGLE OF ATTACK - INSTRUMENTATION . . . . .	9
4. INFLUENCE OF THE ANGLE OF ATTACK INSTRUMENT MOUNTING ON ITS PERFORMANCE . . . . .	11
4.1 Downwash Effect . . . . .	11
4.2 Correction of Angle of Attack for Downwash . . . . .	11
4.2.1 The electrical analog experiment . . . . .	11
4.2.2 Experimental results . . . . .	15
4.3 Effect of Aircraft Roll and Its Correction . . . . .	23
4.3.1 Roll induced vertical air motions . . . . .	23
4.3.2 Adjusting the angle of attack for the roll of the aircraft . . . . .	25
5. FINAL CORRECTED EQUATION FOR VERTICAL AIR MOTIONS . . . . .	27
5.1 The Equation and Error Estimate . . . . .	27
5.2 Sample Results . . . . .	28
6. CONCLUSION . . . . .	34
ACKNOWLEDGMENTS . . . . .	36
REFERENCES . . . . .	37
APPENDIX A - Zero Setting of Pitch Angle Indicator . . . . .	39

## LIST OF FIGURES

<u>Number</u>	<u>Title</u>	<u>Page</u>
1	The vertical component of relative wind . . . . .	7
2	The airfoil section and associated quantities . . . . .	7
3	Angle of attack sensor mounted under the right wing of T-28 . . . . .	10
4	Closer view of the angle of attack sensor . . . . .	10
5	Flow pattern around an airfoil . . . . .	12
6	Equipment set up for electrical analog experiment . . .	14
7	Circuit diagram for the experiment . . . . .	14
8	Result of the electrical analog experiment. Streamline pattern around the airfoil for an angle of attack of $2.5^\circ$ . . . . .	16
9	Result of the electrical analog experiment. Streamline pattern around the airfoil for angle of attack of $5^\circ$ . . . . .	17
10	Result of the electrical analog experiment. Streamline pattern around the airfoil for angle of attack of $7.5^\circ$ . . . . .	18
11	Result of the electrical analog experiment. Streamline pattern around the airfoil for angle of attack of $10^\circ$ . . . . .	19
12	Angle of downwash as a function of the angle of attack . . . . .	20
13	True angle of attack as a function of the measured angle of attack . . . . .	21
14	Roll of the aircraft . . . . .	24
15	Vertical velocity induced by roll . . . . .	24
16	Adjustment of the angle of attack for roll . . . . .	26
17	A section of the plot showing some of the quantities calculated from T-28 flight data of Flight 183, 22 July 1976 . . . . .	31

LIST OF FIGURES (Cont.)

<u>Number</u>	<u>Title</u>	<u>Page</u>
18	A section of the plot showing some of the quantities calculated from T-28 flight data of Flight 183, 22 July 1976 . . . . .	33

LIST OF TABLES

<u>Number</u>	<u>Title</u>	<u>Page</u>
1	Results from the electrical analog experiment . . . .	22
2	Table showing sample updraft calculations using Sand's method ( $w_{\text{Sand}}$ ) and using angle of attack method ( $w_{\text{Sarma}}$ ) . . . . .	29
3	Pitch and angle of attack in level flight free of vertical air motions . . . . .	40

## 1. INTRODUCTION

Updraft is the name given to a vertically moving air current, usually inside a cloud. (A downward current can be considered as an updraft with negative values.) Updrafts are mainly driven by the force of buoyancy in convective storms. It is known that the higher the updraft velocities in a storm, the more severe it is likely to be. Also studies in cloud physics have shown that updrafts play an important role in the growth of hailstones (Mason, 1962). Hence an accurate measurement of the updraft velocities in various parts of a storm would help to understand the behavior of the storm better.

### 1.1 Techniques for Measuring Vertical Air Motions

Accurate measurement of updraft velocities in cumulus clouds has been a major problem in convective storms research. Several methods have been tried so far. Most of them employ an aircraft as a measuring platform. One method often used is to fly an aircraft at a constant power and attitude setting and use the vertical motions of the aircraft as a reasonable estimate of the vertical air velocity (Auer and Sand, 1966; Lenschow, 1976). This method is not often used for updraft measurements inside vigorous storms because of the risk involved in such a flight procedure. However, based on this approach W. Sand evolved a method to measure updraft velocities using the armored T-28 aircraft of the Institute of Atmospheric Sciences, South Dakota School of Mines and Technology. This method is discussed in Section 1.2.

Another method uses a gust probe to measure the vertical air motions. The gust probe is usually mounted on a boom extending from the nose of the aircraft (Kelly and Lenschow, 1978). Gust probes are essentially fixed or movable vanes that are used to measure the air velocities

perpendicular to the flight path. The movable vane type is similar to the angle of attack sensor to be discussed in Section 3, and it measures the angular deviation of the airstream from the flight direction. The fixed vane type measures the component of the wind perpendicular to the flight direction by measuring the strain produced on the vane mounting. These vanes are mounted in different orientations to get components of wind along mutually perpendicular directions.

Angle of attack of the wing information can be used to calculate updraft velocities (Carlson and Sheets, 1971). This method uses the angle of incidence of the relative wind to the aircraft flight direction, the speed of the aircraft, its rate of climb and attitude information to calculate the vertical component of the wind. How it can be done using the data obtained from T-28 flights is the main topic of this thesis.

A recent development in updraft measurement techniques is the use of Doppler radars. The Doppler radar measures the vertical motion by estimating it from the measured vertical velocities of precipitation particles. This method is still in the research stage (Battan, 1973).

#### 1.2 Updraft Measurements with the Armored T-28 Aircraft (Sand's Method)

The T-28 armored aircraft of the Institute of Atmospheric Sciences, South Dakota School of Mines and Technology is specially modified for penetrating thunderstorms and encountering hail (Johnson et al., 1978). It is equipped to measure different characteristics of the air in its flight path, These data are recorded on magnetic tape by an onboard recorder, Later the magnetic tape is processed using a computer to change the raw data into a usable format. One of the quantities calculated from raw data is updraft velocity and Sand's method has been used for this purpose.

This method uses the rate of climb of the aircraft as an initial estimate of the vertical air motion. It is then corrected for aircraft-induced effects due to variations in indicated air speed and engine manifold pressure. The following equation is used.

$$U = \text{ROC} + ((27 - \text{MAP})92.0 + (\text{IAS} - 140)17.7) \cdot (0.00508) \quad (1)$$

where  $U$  = updraft velocity in  $\text{m sec}^{-1}$

$\text{ROC}$  = rate of climb in  $\text{m sec}^{-1}$

$\text{MAP}$  = engine manifold pressure in inches of mercury

$\text{IAS}$  = indicated air speed in knots.

This equation was empirically determined from data obtained from a test flight conducted for that purpose on 28 July 1972. The values 27 and 140 in (1) represent nominal reference values for manifold pressure and indicated air speed respectively. The accuracy of the equation is not specifically known, even though the updraft values thus determined were believed to be within about  $2 \text{ m sec}^{-1}$  (Sand, 1974).

### 1.3 The Angle of Attack Method of Determining Updraft Speeds

The angle of attack method discussed in this thesis uses measurements of the angle of attack of the wing to help determine vertical air motions. It is an analytical method which has the advantage over the empirical method mentioned in Section 1.2 that it is not influenced by any particular set of field conditions. Also if the accuracies of the instruments are known, the net accuracy in updraft measurement can be estimated.

This method using the angle of attack was not used before, mainly because the angle of attack sensor was not available on the T-28 until 1976. Also as the T-28 is a single engined aircraft the sensor cannot



be mounted using a noseboom so that it will be free from any aircraft-induced flow effects. Mounting it elsewhere on the aircraft requires the use of equations to take into account the induced airflow effects.

2, THE BASIC THEORY BEHIND UPDRAFT CALCULATIONS  
USING THE ANGLE OF ATTACK METHOD

Updraft velocity can be thought of as the vertical component of the absolute wind vector (i.e. relative to the terrestrial frame of reference). As the measurements of the different quantities involved are made using an aircraft, the air motion is divided into

- i) the motion of the aircraft and
- ii) the motion of the air relative to the aircraft.

So

Velocity of air = Velocity of aircraft + velocity of air relative  
to the aircraft.

$$\text{i.e. } V = V_{a/c} + V_{rel} \quad (2)$$

where  $V$  = velocity of air

$V_{a/c}$  = velocity of aircraft

$V_{rel}$  = velocity of air relative to the aircraft.

Taking vertical components on both sides of (2),

$$k \cdot V = k \cdot V_{a/c} + k \cdot V_{rel} \quad (3)$$

where  $k$  is a unit vector in the vertical.

This is equivalent to saying that

$$\text{Updraft velocity} = \text{Vertical speed of the aircraft} + \text{vertical} \\ \text{airspeed relative to the aircraft} \quad (4)$$

Using the symbol  $w$  for vertical velocities

$$w' = w_{a/c} + w_{rel} \quad (5)$$

$w'$  is used to denote vertical velocity not corrected for roll motion of the aircraft. This correction is done in a later section.

The vertical speed of the aircraft is given by the rate of climb

$$w_{a/c} = \text{rate of climb}$$

In the T-28 it is usually obtained by differentiating the altitude of the aircraft with respect to time. A source of back-up rate of climb data is provided by a variometer. So to get the updraft velocity it suffices to calculate the vertical velocity of air relative to the aircraft, i.e. the vertical component of the relative wind.

Let  $\gamma$  denote the angle in the vertical plane between the relative wind and the horizontal plane (see Fig. 1). Then,

$$\text{Vertical component of the relative wind} = \text{Relative wind speed} \cdot \text{Sine } \gamma$$

$$\text{i.e. } w_{\text{rel}} = |V_{\text{rel}}| \cdot \text{Sin } \gamma \quad (6)$$

$|V_{\text{rel}}|$  is very closely equal to the true air speed of the aircraft. The angle of attack,  $\alpha$ , gives the angle between the relative wind and the chord line of the wing, considered positive in the sense shown in Fig. 2. The angle of  $\alpha$  is measured in a plane perpendicular to the lateral axis of the aircraft. The angle of pitch  $\theta$  gives the angle between the aircraft's longitudinal axis, which very closely approximates the direction of flight in balanced conditions, and the horizontal plane. It is measured in the vertical plane (ref. Appendix A for zero correction of pitch angle). The angle of incidence of chord,  $\delta$ , is the angle between the chord line in question and the longitudinal axis of the aircraft. (In this discussion  $\delta$  would denote the angle of incidence of the chord at the wing station where the angle of attack sensor is mounted.)

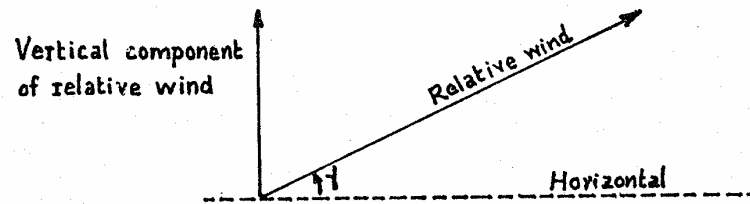


Fig 1: The vertical component of relative wind.

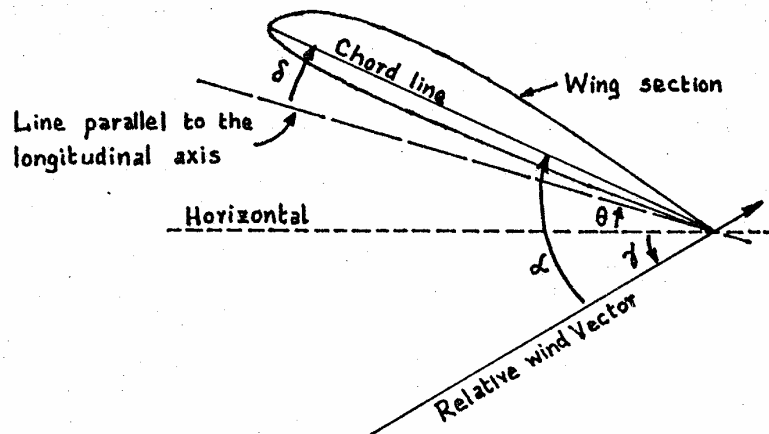


Fig 2: The airfoil section and associated quantities.

It is clear from Fig. 2 that

$$\gamma = \alpha - \theta - \delta \quad (7)$$

So (6) becomes

$$w_{rel} = |V_{rel}| \cdot \sin(\alpha - \theta - \delta)$$

Equation (5) can hence be rewritten as

$$w' = w_{a/c} + |V_{rel}| \cdot \sin(\alpha - \theta - \delta) \quad (8)$$

This is the main process involved even though there are complexities in measuring some of the quantities.

### 3. MEASURING THE ANGLE OF ATTACK - INSTRUMENTATION

The instrumentation to measure the T-28 angle of attack consists of an "angle of attack sensor" and an onboard recording facility. The sensor is a movable vane, mounted in such a way that the vane rotates about an axis parallel to the lateral axis of the aircraft (see Figs. 3 and 4). On the T-28 the sensor is mounted beneath the right wing at a distance of 3.84 meters (12.5 feet) from the longitudinal axis. The axis of rotation of the vane is 0.23 meters (9 inches) below the lower surface of the wing (see Fig. 3).

The vane aligns itself to the airstream at that point and the angular displacement of the vane from a reference position is measured electronically and records on magnetic tape by the onboard recorder. The angular travel range of the vane is  $52.6^\circ$ . The reference line chosen is a line through the pivot point of the vane parallel to the chordline at the wingstation where the instrument is mounted. The vane can travel  $29.4^\circ$  above the reference line and  $23.2^\circ$  below. The angle measured is positive when the vane is above the reference line, negative when below and is referred to as the "measured angle of attack"  $\alpha'$ . As will be seen later  $\alpha'$  differs from  $\alpha$ , the true angle of attack.

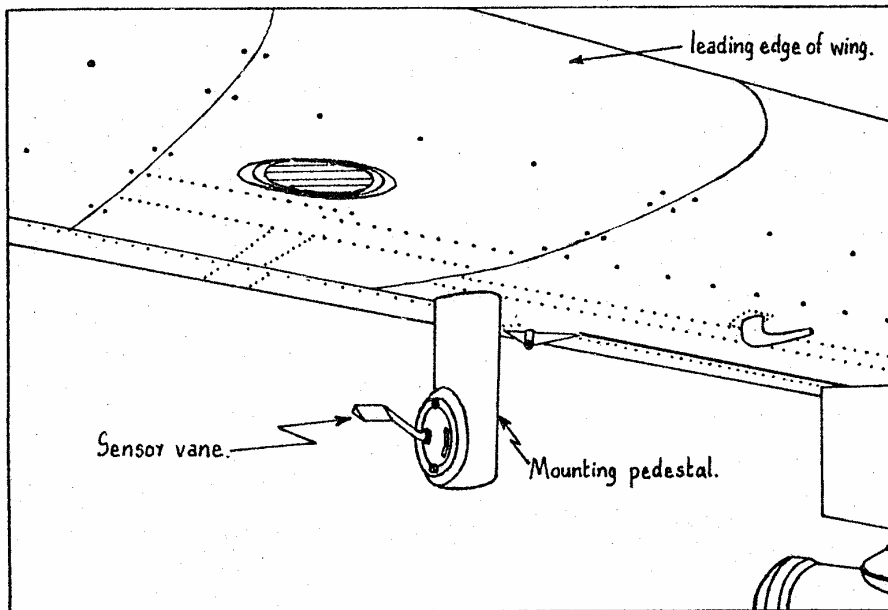


Fig 3 : Angle of attack sensor mounted under the right wing of T-28.

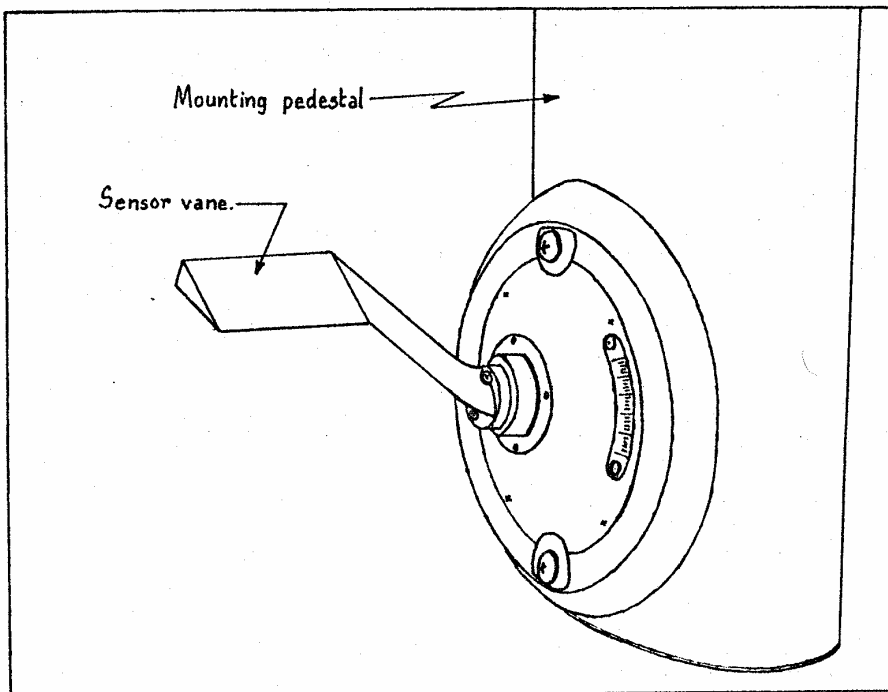


Fig: 4 : Closer view of the angle of attack sensor.

#### 4. INFLUENCE OF THE ANGLE OF ATTACK INSTRUMENT

##### MOUNTING ON ITS PERFORMANCE

#### 4.1 Downwash Effect

As was mentioned in Section 3, the angle of attack sensor is mounted beneath the right wing of the T-28, 0.23 meters (9 inches) below the lower surface of the wing. According to Newton's third law of motion the airfoil gives lift because it imparts a downward momentum to the air through which it moves. This would change the direction of the airflow mainly behind the leading edge of the airfoil (Carter, 1929, page 181), in the immediate vicinity of the wing. This implies that at the location of the angle of attack sensor vane the airstream direction is different from the relative wind vector (Fig. 5).

The angular deflection of the streamlines due to the effect of the airfoil at a particular point is called the "angle of downwash" at that point. Let  $\alpha'$  denote the measured angle of attack. Then the true angle of attack is given by

$$\alpha = \alpha' + \epsilon \quad (9)$$

where  $\epsilon$  denotes the angle of downwash at the location of the vane.

#### 4.2 Correction of Angle of Attack for Downwash

Correcting the measured angle of attack for the downwash effect involves computing the angle of downwash for different angle of attack settings to find an algebraic expression which gives the corrected angle of attack as a function of the measured angle of attack.

##### 4.2.1 The electrical analog experiment

To find the angle of downwash for different angles of attack, an electrical analog experiment which very closely simulates the airflow



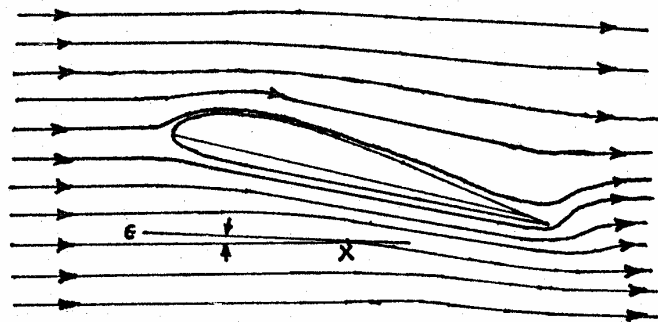


Fig 5. Flow pattern around an airfoil.  $\epsilon$  is the angle of downwash at the point X.

around the airfoil was conducted. Electrical analog experiments are generally used to simulate fluid flow in tubes, flow around airfoils, heat transfer through a medium, etc. These experiments simulate the fluid flow using an electric field, which needs the assumption that the flow is incompressible (Shapiro, 1953). This is a reasonable assumption here because in stable flight conditions the flow around the airfoil is streamlined and there is no flow separation.

The basic principle of the experiment is to apply an electrical potential across the length of a piece of "conducting paper," which has a hole cut out of it in the shape of the airfoil section under investigation. (The conducting paper is paper coated with an electrically conducting material like graphite.) The potential is applied in a direction parallel to the mean flow. The equipotential lines are traced and from them the streamlines are derived.

The equipment consists of the conducting paper, aluminum foil electrodes, a potential divider and power source, a galvanometer and probe to find zero potential points on the conducting paper and connection wires.

A rectangular piece of conducting paper was taken and aluminum foil strips were attached along the breadths of the paper, using silver paint to ensure good contact with the paper (see Fig. 6). For better results an uninsulated copper wire was embedded throughout the length of each of the aluminum foil electrodes. Then a hole was cut in the middle of the paper in the shape of an airfoil such that the chordline made an angle equal to the desired angle of attack, with a line perpendicular to the electrodes. To cut the hole a template which was a scale model of the

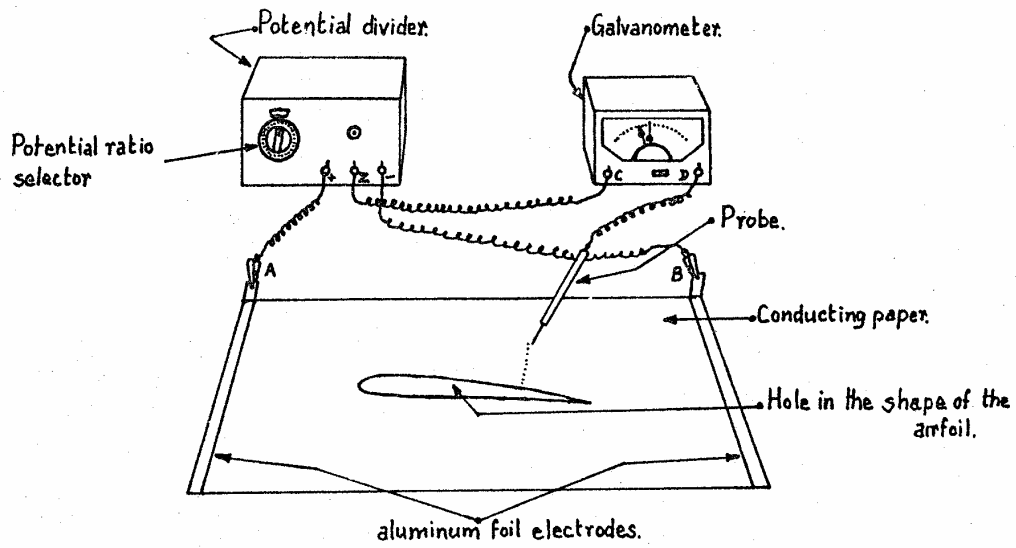


Fig. 6 : Equipment set up for electrical analogue experiment.

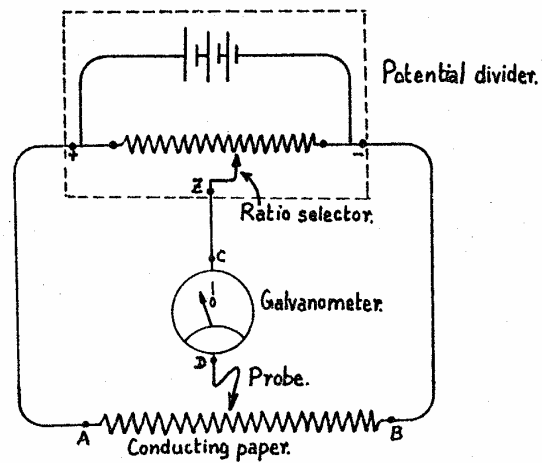


Fig: 7 : Circuit diagram for the experiment.

section of the wing of the T-28 at the wingstation where the angle of attack sensor is mounted was used.

The potential was applied with the help of the potential divider so that one electrode was at a positive potential and the other at a negative potential. The potential divider was then adjusted so that the zero potential line divides the length of the paper in a suitable ratio. The galvanometer was connected between the zero potential terminal of the potential divider and the probe (see Fig. 7). Using the probe the position of the zero potential line on the paper was found. This was done by sliding the probe along the length of the paper until the galvanometer read zero. A set of points thus found help to trace the line. The process was repeated with different potential settings. It is clearly seen that the lines thus obtained are equipotential lines.

Streamlines are then obtained by drawing a set of lines orthogonal to the equipotential lines. The angle of downwash at the location of the vane is obtained by measuring the angle made by the streamline through that location with a line perpendicular to the electrodes.

#### 4.2.2 Experimental results

The experiment was repeated with different angles of attack. The streamline patterns thus obtained are reproduced in Figs. 8, 9, 10, and 11. The results are tabulated in Table 1. The results were then plotted on graph paper and a smooth curve was sketched through the data points (see Fig. 12). This curve was checked with the downwash angle curve given on Fig. 139 of Carter (1929). They were found to be of the same general shape and trend. Figure 13 gives the true angle of attack versus measured angle of attack.

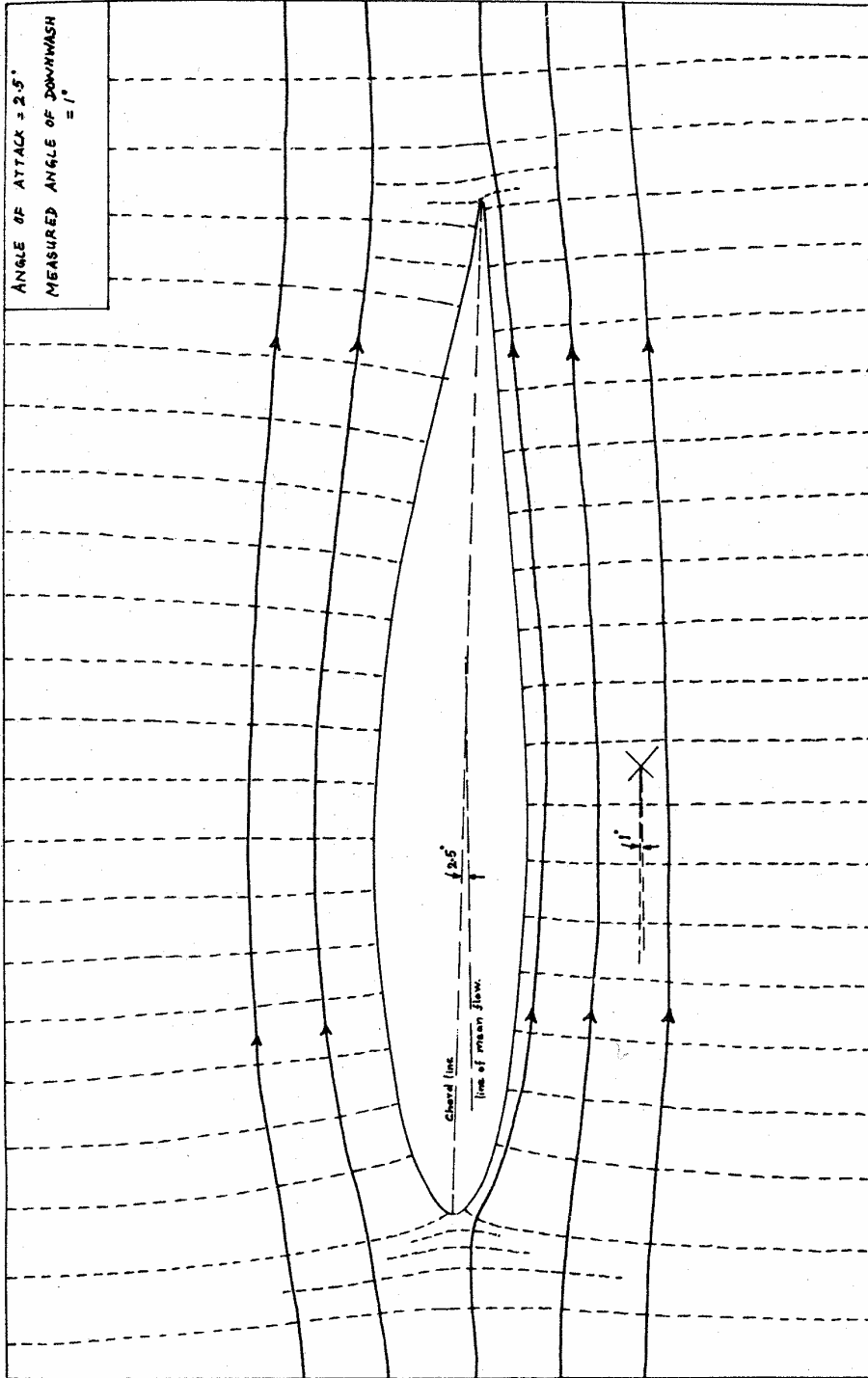


Fig 8 . Result of the electrical analog experiment.  
Streamline pattern around the airfoil for an angle of attack of  $2.5^\circ$

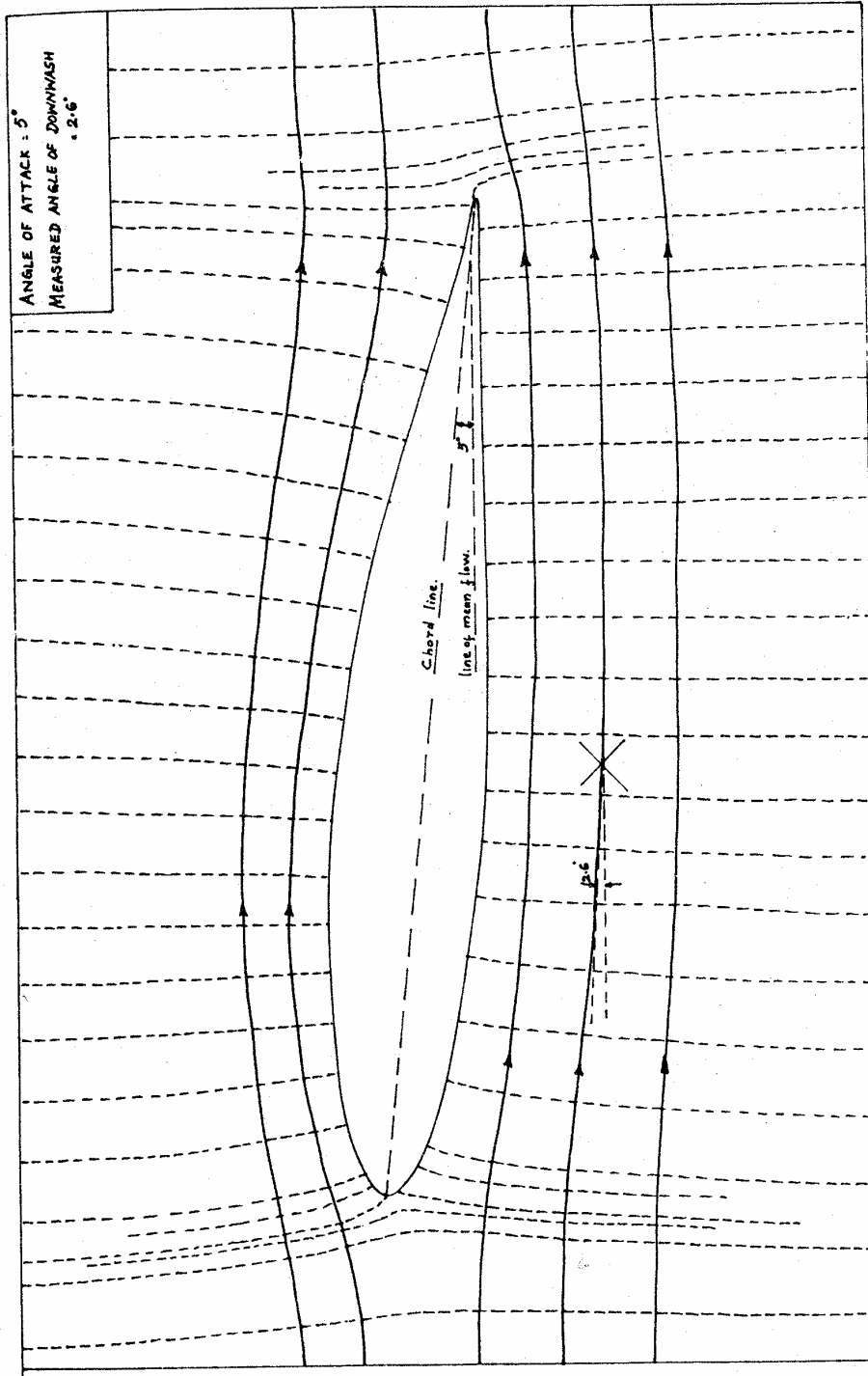


Fig 9. Result of the electrical analog experiment.  
 Streamline pattern around the airfoil for angle of attack of  $5^\circ$

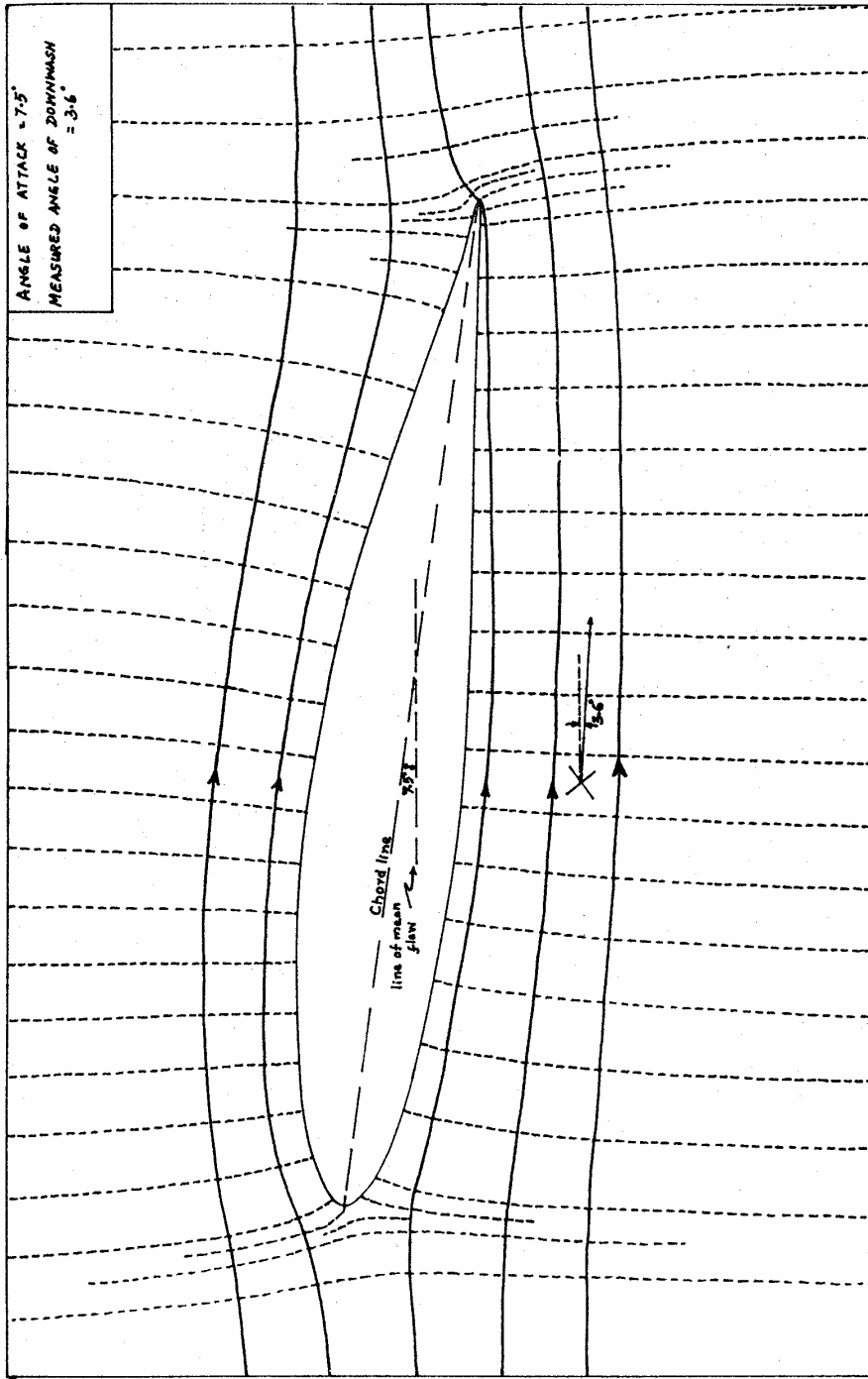


Fig 10. Result of the electrical analog experiment.  
Streamline pattern around the airfoil for angle of attack of 7.5°

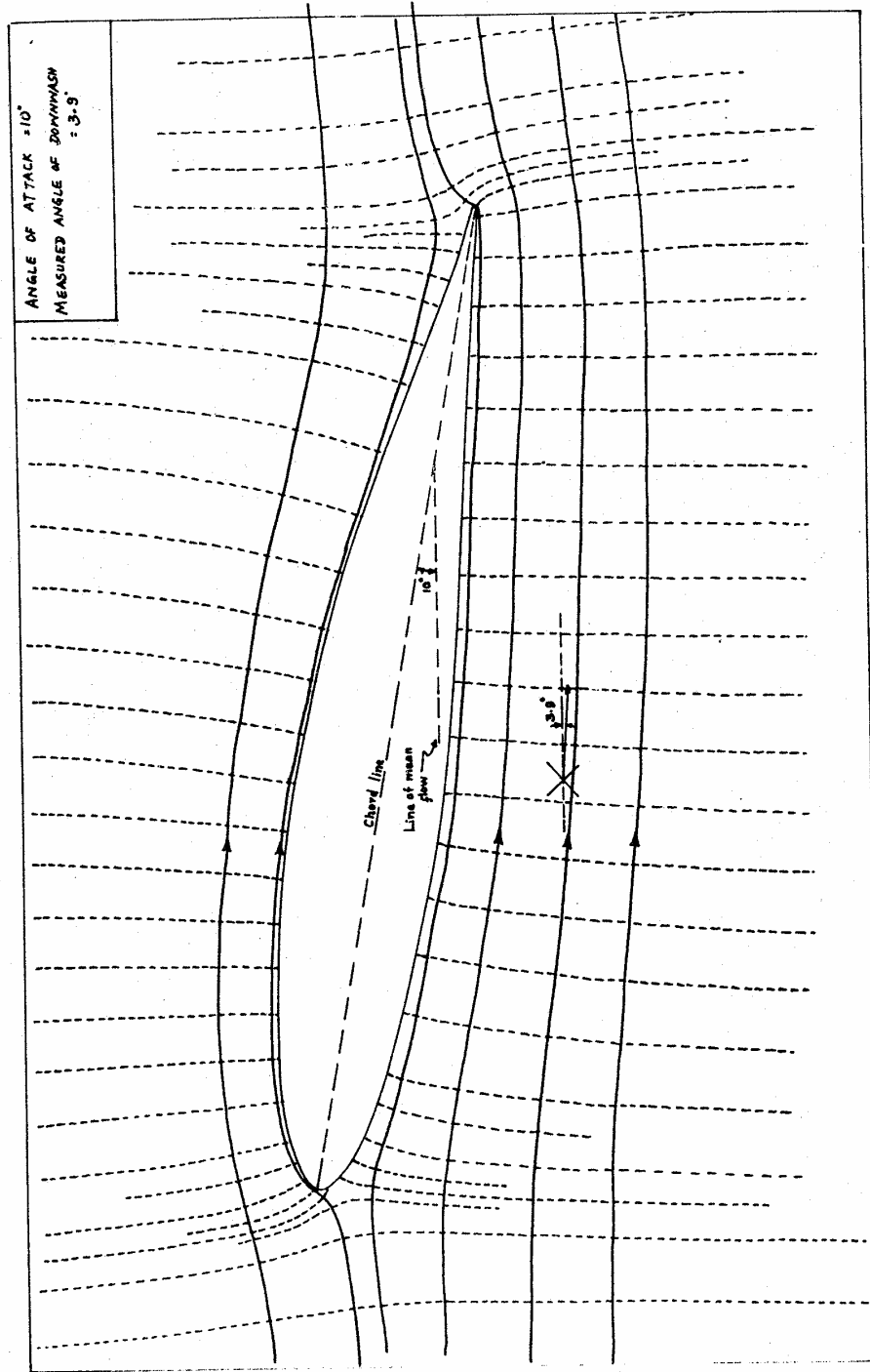


Fig 11. Result of the electrical analog experiment  
 Streamline pattern around the airfoil for angle of attack of  $10^\circ$



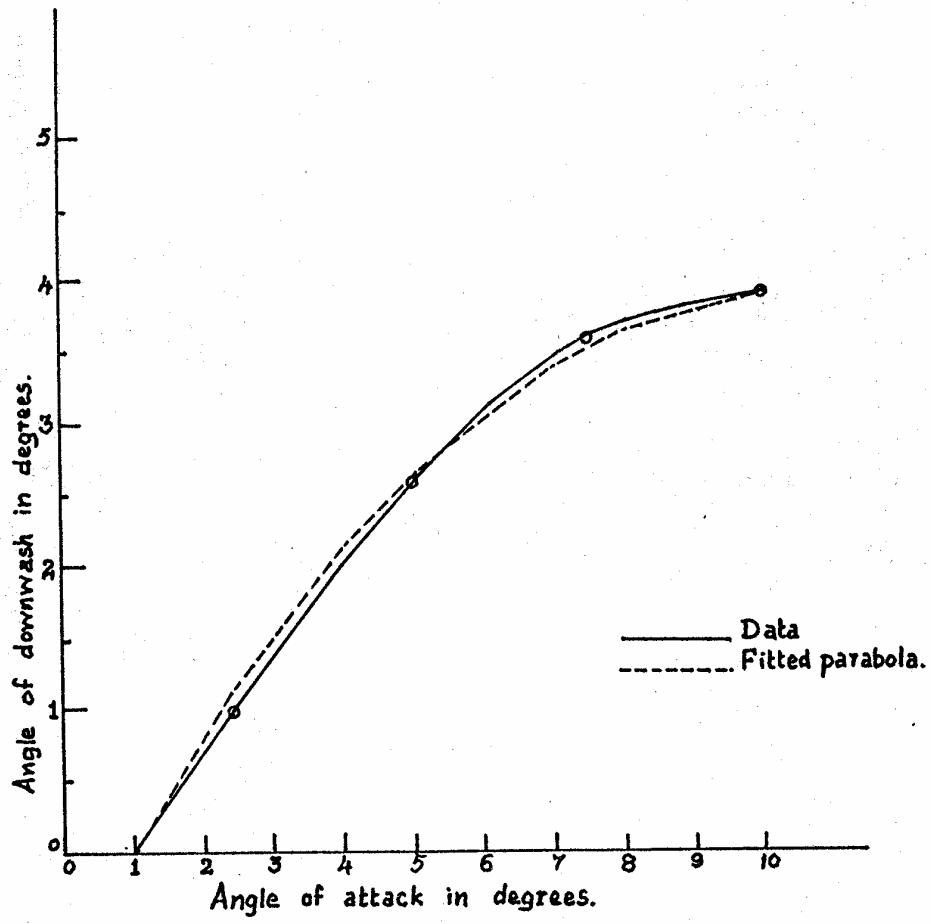


Fig 12: Angle of downwash as a function of the angle of attack.

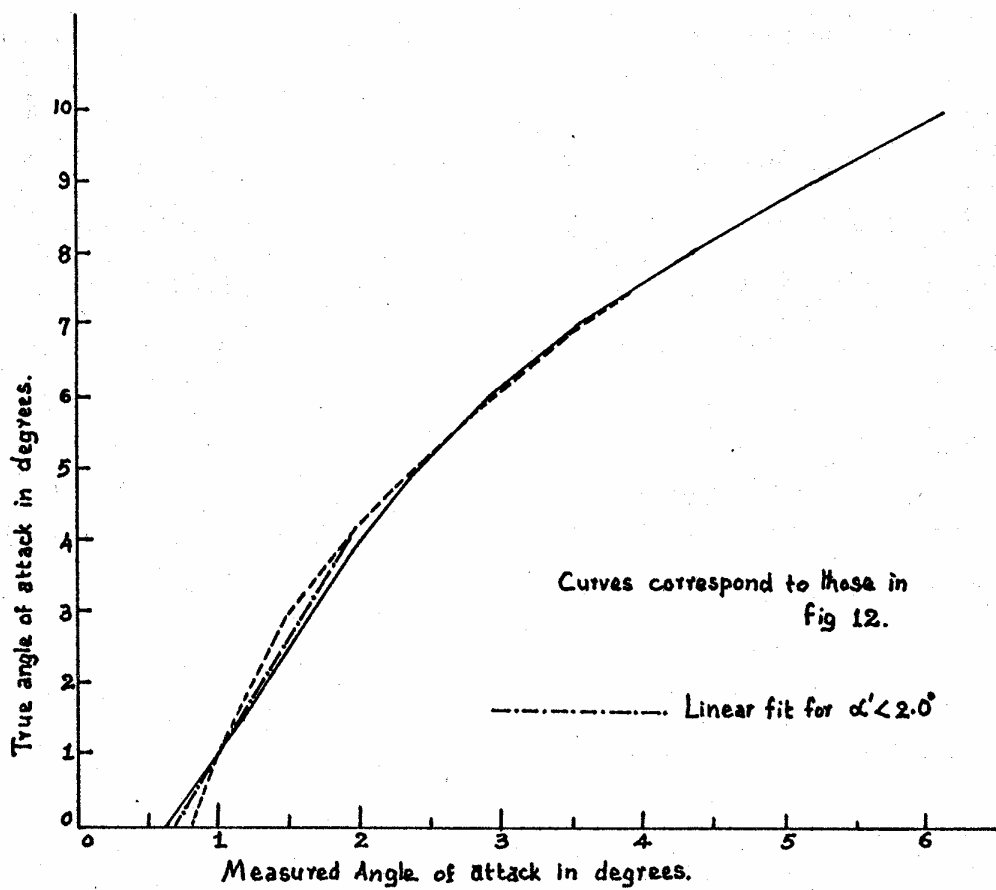


Fig 13. True angle of attack as a function of the measured angle of attack.

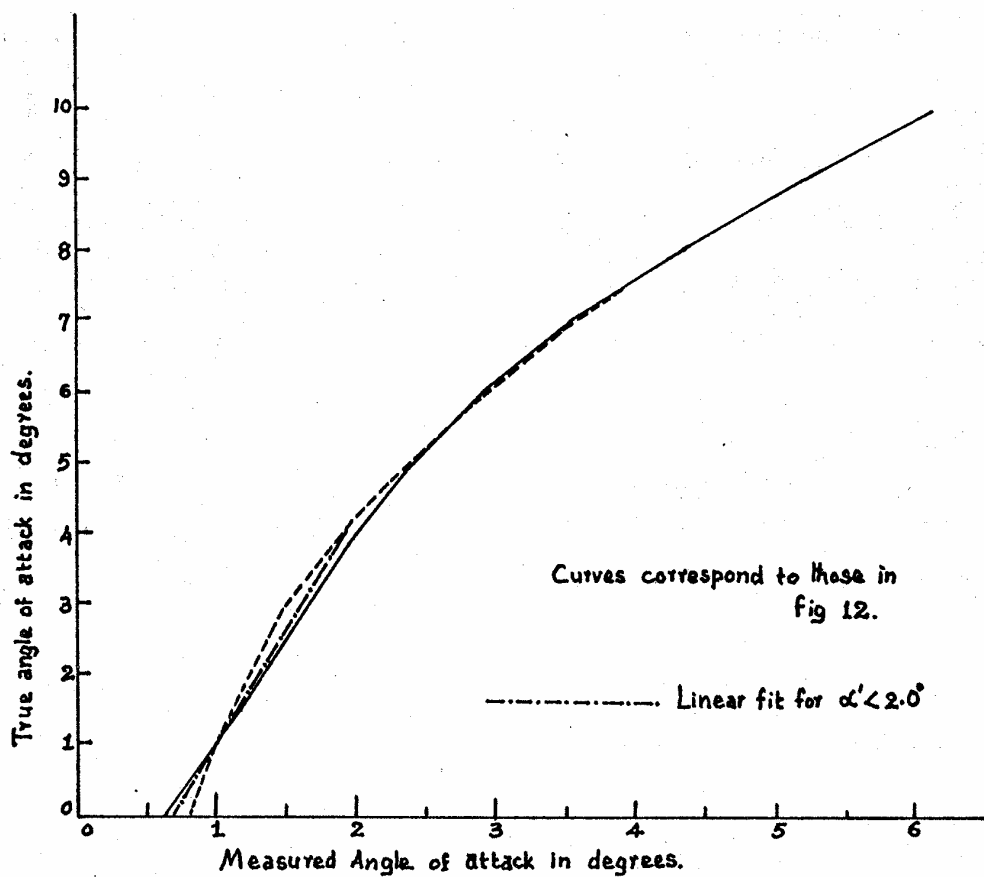


Fig 13. True angle of attack as a function of the measured angle of attack.

TABLE 1

Results from the electrical analog experiment

<u>Angle of attack in degrees</u>	<u>Angle of downwash in degrees</u>
2.5	1.0
5.0	2.6
7.5	3.6
10.0	3.9

To get an analytical equation to represent the curve in Fig. 12, a parabola was fitted to the set of data points and was found to fit well in the range of  $0^\circ < \alpha < 10^\circ$ , where  $\alpha$  represents the true angle of attack (correlation coefficient between the data points and the fitted parabola = 0.99). The parabola thus fitted is sketched in by broken line in Fig. 12.

Thus the equation connecting angle of attack and angle of downwash for the T-28 is

$$\epsilon = -0.044\alpha^2 + 0.914\alpha - 0.869 \quad (10)$$

From (9)

$$\alpha = \alpha' + (-0.044\alpha^2 + 0.914\alpha - 0.869)$$

Solving this for  $\alpha$  we get

$$\alpha = -0.977 \pm (22.727\alpha' - 18.853)^{\frac{1}{2}} \quad \text{for } \alpha' \geq 0.83^\circ$$

On checking with Fig. 13 the solution with the positive discriminant was chosen as the other is an extraneous root of the quadratic equation.

Restricting the solution for  $\alpha' \geq 2.0^\circ$

$$\alpha = -0.977 + (22.727\alpha' - 18.853)^{\frac{1}{2}} \quad \text{for } \alpha' \geq 2.0^\circ \quad (11)$$

From Fig. 13 it can be seen that for low values of  $\alpha'$  the curve becomes almost a straight line. So a linear relation was assumed for values of  $\alpha'$  less than  $2.0^\circ$

$$\alpha = -2.18 + 3.18\alpha' \quad \text{for } \alpha' < 2.0^\circ \quad (12)$$

Equations (11) and (12) are combined and illustrated in Fig. 13 by the broken line. Both  $\alpha$  and  $\alpha'$  in (11) and (12) are in degrees.

#### 4.3 Effect of the Aircraft Roll and Its Correction

Roll is the rotary motion of the aircraft about its longitudinal axis (see Fig. 14). The angular displacement thus produced measured from the horizontal is the angle of roll  $\beta$ . The angle of roll is considered positive for counterclockwise rotation when viewed from the front end of the aircraft, and negative for clockwise rotation.

##### 4.3.1 Roll induced vertical air motions

As the aircraft rolls a vertical velocity  $w_{\text{roll}}$  is induced at the location of the angle of attack sensor, which is given by

$$w_{\text{roll}} = r \frac{d\beta}{dt} \quad (13)$$

where  $r$  is the distance between the vane and the longitudinal axis of the aircraft, and  $\beta$  is given in radians.

As the vane is mounted beneath the right wing of the T-28, a positive roll would increase the relative updraft velocity (see Fig. 15) so that

$$w = w' - w_{\text{roll}}$$

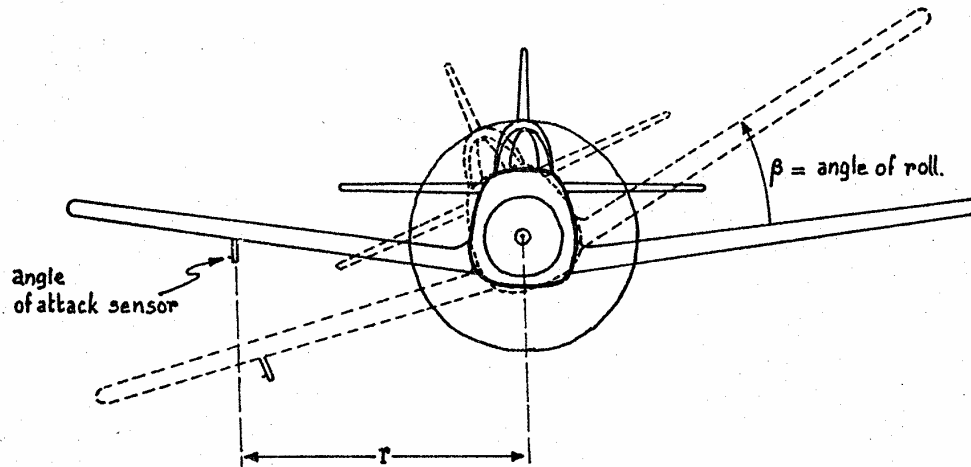
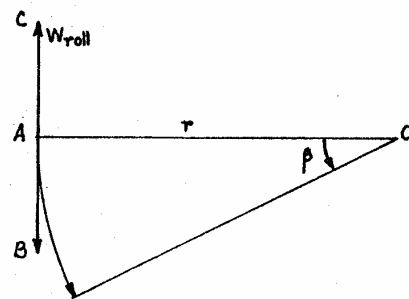


Fig 14 : Roll of the aircraft.



$\vec{AB}$  = linear velocity induced by roll.  
 $\vec{AC}$  = apparent vertical velocity of air.

Fig 15: Vertical velocity induced by roll.

where  $w'$  is given by (8). When this correction is applied (8) becomes

$$w = w_{a/c} + |V_{rel}| \cdot \sin(\alpha - \theta - \delta) - r \frac{d\beta}{dt} \quad (14)$$

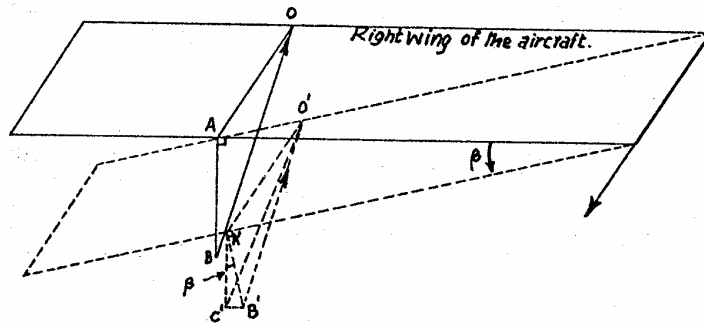
But as shown in Section 5.1 the magnitude of this correction is typically small.

#### 4.3.2 Adjusting the angle of attack for the roll of the aircraft

It is evident from Figs. 1 and 2 that to get the vertical component of the relative wind the angles involved, i.e. the angle of attack and angle of pitch, should be measured in the vertical plane. As the pitch angle is measured by a system which uses the vertical as a reference, only the angle of attack need be corrected for deviations from the vertical. The angle of attack, as seen in Section 3, is measured in a plane perpendicular to the lateral axis and parallel to the longitudinal axis of the aircraft. So when the angle of roll is equal to  $\beta$ , this plane is inclined to the vertical at an angle  $\beta$ . From the geometry of Fig. 16, the projection of the angle of attack  $\alpha$  in a plane passing through the side O'A' of the angle and making an angle  $\beta$  with the plane of  $\alpha$  is given by

$$\alpha_p = \text{Arc tan}(\tan \alpha \cdot \cos \beta) \quad (15)$$

where  $\alpha_p$  represents the projection of  $\alpha$  on a vertical plane parallel to the longitudinal axis of the aircraft.



$OB, O'B'$  - relative wind vectors through the axis of rotation of the vane  
and perpendicular to it.

Broken outline represent wing position after roll.

$$\angle B'O'A' = \alpha ; \quad \angle C'O'A' = \alpha_p$$

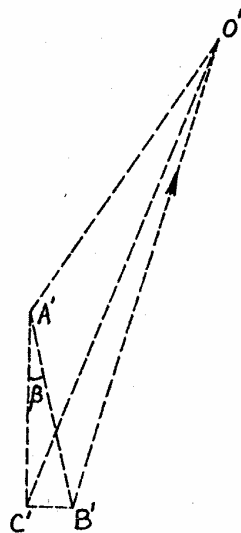


Fig 16. Adjustment to the angle of attack for roll.

$$\begin{aligned} \tan \alpha_p &= \frac{C'A'}{O'A'} = \frac{C'A'}{B'A'} \cdot \frac{B'A'}{O'A'} \\ &= \cos \beta \cdot \tan \alpha \end{aligned}$$



## 5. THE FINAL CORRECTED EQUATION FOR VERTICAL AIR MOTIONS

### 5.1 The Equation and Error Estimate

Equation (8) says that

$$w' = w_{a/c} + |V_{rel}| \cdot \sin(\alpha - \theta - \delta)$$

As the angle of attack is not measured in the vertical plane  $\alpha$  is replaced by  $\alpha_p$  which is given by (15). Including the effect of the roll rate

$$w = w_{a/c} + |V_{rel}| \cdot \sin(\alpha_p - \theta - \delta) - r\dot{\beta} \quad (16)$$

where  $\dot{\beta} = \frac{d\beta}{dt}$  radians/sec

$$\alpha_p = \arctan(\tan\alpha \cdot \cos\beta)$$

$$\alpha = -0.977 + (22.727\alpha' - 18.853)^{1/2} \quad \text{for } \alpha' \geq 2.0^\circ$$

$$\alpha = -2.18 + 3.18\alpha' \quad \text{for } \alpha' < 2.0^\circ$$

$$r = 3.8 \text{ meters} \quad \text{for the T-28}$$

$$\delta = 0.5^\circ \quad \text{for the T-28}$$

The vertical velocity of the aircraft normally ranges from -20 to +20 m sec<sup>-1</sup>. Typical magnitudes of the quantities in (16) are,

$$|V_{rel}| = \text{True air speed} \approx 100 \text{ m sec}^{-1}$$

$$|\alpha_p - \theta - \delta| \approx 4^\circ$$

$$|\dot{\beta}| \approx 3^\circ \text{ sec}^{-1} = 0.052 \text{ radians sec}^{-1}$$

$$||V_{rel}| \cdot \sin(\alpha_p - \theta - \delta)| \approx 7 \text{ m sec}^{-1}$$

$$|r\dot{\beta}| \approx 0.25 \text{ m sec}^{-1}$$

Hence the correction term due to relative motion of air with respect to the aircraft can amount to one-third or more of the measured updraft speed. The roll rate correction can usually be neglected as it is only about 2% of the total.

In the T-28 the basic recorded data accuracies of pitch and roll angles are  $\pm 0.15^\circ$ . The total accuracy of the quantity  $(\alpha - \theta - \delta)$  after considering the uncertainty due to downwash and the curve fit (refer to Section 4.2.2) would be about one degree. The true air speed is estimated to be within 0.2%. Hence the second term in (16) is correct to  $\pm 2 \text{ m sec}^{-1}$ . The rate of climb error is less than  $3 \text{ m sec}^{-1}$ . So the total uncertainty in the updraft speeds is less than  $5 \text{ m sec}^{-1}$ . It should be noted that this is an extreme value.

The quality of this equation can be improved considerably by increasing the accuracy of the rate of climb values. This equation is free from any environmental influences and hence can be used in any stable flight conditions.

## 5.2 Sample Results

Table 2 gives some of the different quantities, measured using the T-28, that go into updraft calculations. Each row corresponds to a particular time during the flight and they have been selected from the data acquired during cloud penetrations on 22 July 1976. (They do not constitute a continuous time interval.) The sample data have been divided into three sections:

- a) for large rate of climb values with rate of climb greater than zero.
- b) rate of climb small in magnitude.
- c) rate of climb large in magnitude but negative in sign.

$w_{\text{Sand}}$  and  $w_{\text{Sarma}}$  give the updraft velocities calculated using Sand's method and the angle of attack method respectively (i.e.  $U$  in (1) and  $w$  in (16)). They are not found to agree very well. The values

TABLE 2  
 Table Showing Sample Updraft Calculations Using Sand's Method  
 ( $w_{\text{Sand}}$ ) and Using Angle of Attack Method ( $w_{\text{Sarma}}$ )

	Time	IAS (kts)	TAS (kts)	MAP ("of Hg)	$\alpha_p$ (deg)	$\theta$ (deg)	$\beta$ (deg)	$d\beta/dt$ (deg s <sup>-1</sup> )	ROC (m s <sup>-1</sup> )	$w_{\text{Sand}}$ (m s <sup>-1</sup> )	$w_{\text{Sarma}}$ (m s <sup>-1</sup> )
A	163154	128.4	180.0	27	2.26	5.75	-17	0	-5.6	-6.7	-12.1
	164130	138.3	199.2	24	4.15	-0.25	-21	2	-16.8	-15.6	-10.0
	165808	125.0	181.8	25	6.38	2.75	-1	-2	-11.3	-11.6	-6.1
	171529	129.9	182.5	26	6.38	-7.25	-1	2	-19.2	-19.7	2.1
	170700	133.2	184.5	28	6.70	4.75	2	1	-9.0	-10.0	-6.7
B	163312	123.0	181.2	24	2.53	1.75	1	9	0.2	0.1	0.1
	164057	121.4	177.3	25	4.66	-0.25	-15	0	0.8	0.2	7.8
	165839	133.7	192.7	25	5.82	4.75	-2	2	0.1	0.2	1.0
	171513	115.6	163.8	25	5.09	3.75	7	6	2.5	1.2	3.3
	165721	111.2	163.9	24	4.18	4.75	1	-6	1.7	0.7	0.5
C	163253	125.5	184.0	25	-0.17	1.75	0	-6	15.8	15.8	7.3
	163300	130.8	189.4	25	-2.92	0.75	0	1	18.8	19.0	11.7
	164040	138.3	198.9	26	1.50	10.75	2	2	24.5	24.7	7.9
	171444	119.9	167.4	27	5.95	7.75	14	-5	18.3	16.7	18.6
	165700	146.6	212.5	27	1.26	4.75	3	-2	17.4	18.2	9.9

Note:  $\theta$  and  $\alpha$  have been adjusted for zero correction.

calculated from the angle of attack method are generally smaller in magnitude than those from Sand's method, when the latter reach  $10 \text{ m sec}^{-1}$  or more.

It is worth noting the situation described by the fourth row of Section A in Table 2 corresponding to time 17:15:29 (ref. Fig. 17 for data plot).

$$w_{\text{Sand}} = -19.7 \text{ m sec}^{-1}$$

$$w_{\text{Sarma}} = +2.1 \text{ m sec}^{-1}$$

At this time the aircraft was pitched downward ( $\theta = -7.25^\circ$ ), yet the angle of attack was positive ( $\alpha_p = 6.28^\circ$ ). The aircraft started pitching down at time 17:15:03 (ref. Fig. 17) and continued in that attitude until 17:15:27. Then it is pitched up until 17:15:36. The vertical velocity calculated from (1),  $w_{\text{Sand}}$ , shows a downdraft region exactly in the same time period and the extreme values of pitch and  $w_{\text{Sand}}$  in that period occur almost simultaneously. It is clear from these indicators that a major portion of the negative rate of climb or downward motion was due to the attitude of the aircraft. The angle of attack method of calculation reflects this fact, as  $w_{\text{Sarma}}$  does not show a prominent downdraft in that region, whereas the Sand method does not.

Sand's method has been observed to give updraft values very close to the aircraft rate of climb. This is because the corrections applied to the rate of climb are small in magnitude in (1). Sand's method assumes that the T-28 attitude remains fairly constant and that the aircraft's motion would mainly be decided by the updrafts and downdrafts. It takes into account the changes in vertical motion due to changes in engine power and indicated air speed, but fails to consider the changes brought about by variations in the angle of pitch and angle of attack.

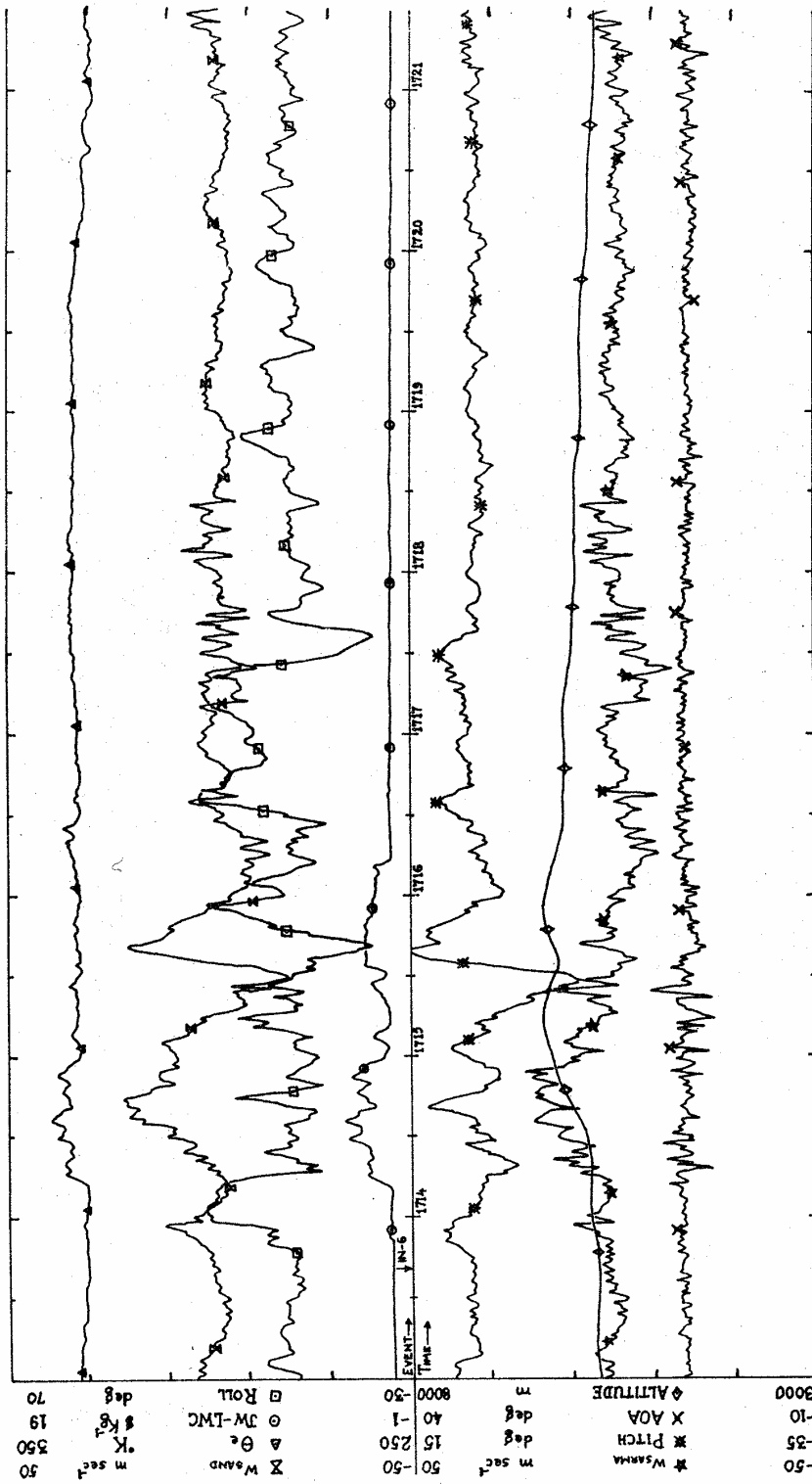


Fig 17. A section of the plot showing some of the quantities calculated from T-28 flight data of Flight 183, 22 July 1976. The scales used are shown on the left hand side. Time is given on the central line.

Vertical air velocities computed from (16) have a tendency to show small downdrafts of perhaps 3 or 4 m sec<sup>-1</sup> after the end of a cloud penetration, i.e. the regions between penetrations appear to be dominated by small downdrafts even though the aircraft may be well outside the cloud. Figure 18 shows an example of this in the time period after about 16:33:15. This downward shift in vertical air velocities was also accompanied by a downward shift in the angle of attack values. The average value of the angle of attack soon after the end of the penetration was less than the value before the penetration (ref. Fig. 18). This behavior of the angle of attack trace suggests the possibility of icing on the angle of attack sensor vane. The vane is electrically heated for deicing purposes, but the amount of heating may be inadequate. If ice builds up on the vane, the weight of the ice would push the vane down, thus lowering the measured angle of attack. This in turn would decrease the updraft values computed from (16). After the end of a penetration the average angle of attack value tries to come up a little possibly as the ice melts off the sensor vane.

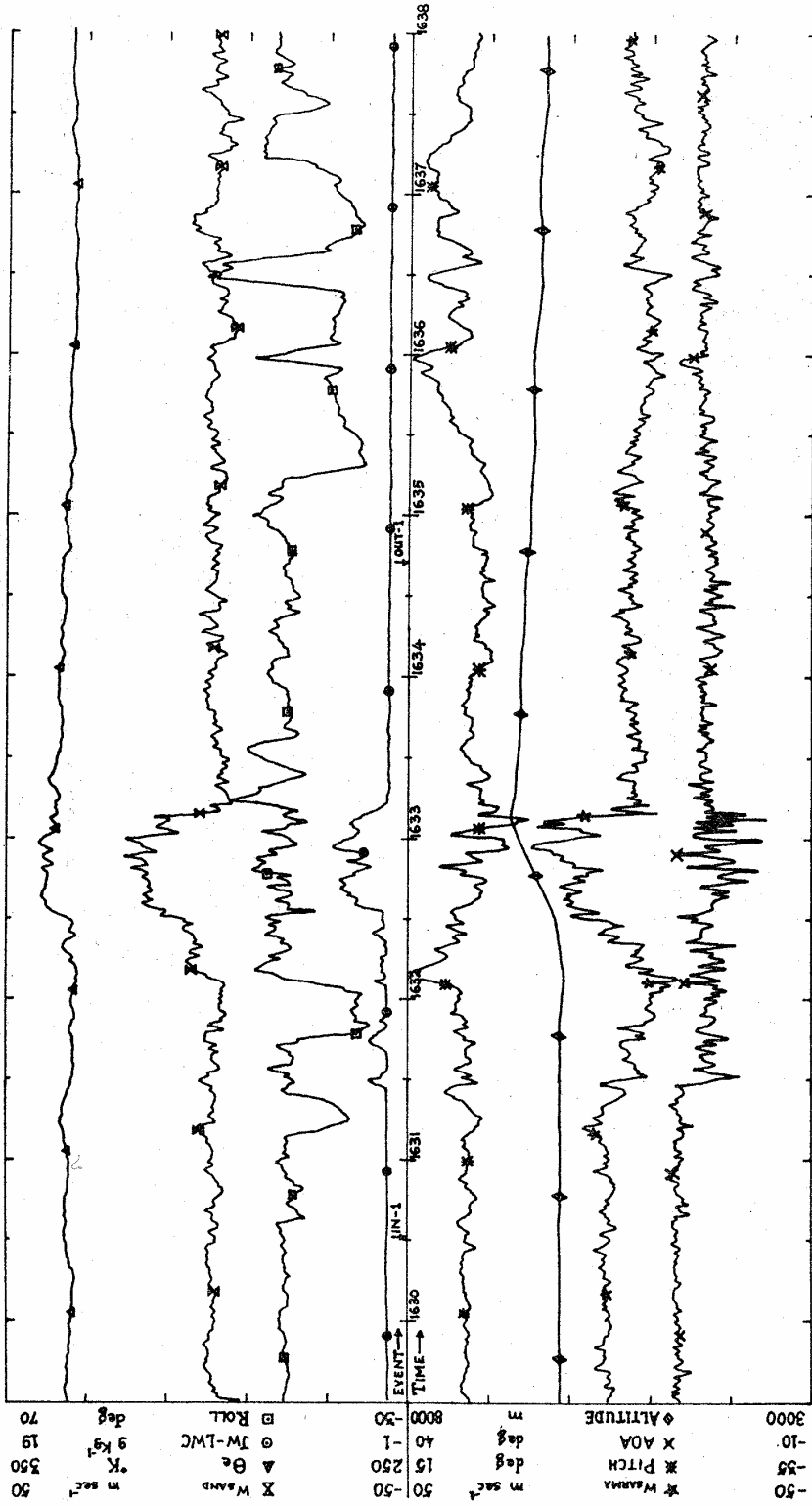


Fig 18. A section of the plot showing some of the quantities calculated from T-28 flight data of Flight 183, 22 July 1976. The scales used are shown on the left hand side. Time is given on the central time.

## 6. CONCLUSION

The new updraft equation (16) appearing in Section 5.1 has been designed to overcome some of the drawbacks of (1) mentioned in Section 1.2. As was seen earlier, (1) was derived in an empirical manner from data obtained from a test flight of the T-28 flown for that purpose (Sand, 1974). This puts a serious limitation to the equation in that it cannot be assumed to be completely valid in conditions different from the one in which the test flight was conducted. In other words there could be other factors governing the aircraft's motion, which were absent in the test flight environment. For example, (1) does not take into consideration the effects that can be produced by a change in aircraft attitude which might be either pilot induced or due to external forces acting on the aircraft.

Equation (16) has been designed to account for these effects so that the deficiency mentioned above is overcome. It takes into account the changes in aircraft attitude like roll and pitch angle changes. Like (1), (16) also uses the rate of climb of the aircraft as a first estimate of the vertical air motion and applies corrections to it depending on the changes of the flight characteristics of the aircraft. It was observed that usually these corrections were larger in magnitude than the corrections incorporated into (1).

The main drawback in this work is the fact that there were no data available that could be used as a control, i.e. data regarding a situation for which the updraft values are known to be 100% accurate. This lack of control data makes it impossible to come to a decisive conclusion regarding the new equation. More work could be done to



improve this method. For example to determine the downwash angle a wind tunnel test would give more realistic results. The electrical analog experiment is only an approximation, but a wind tunnel test was not attempted as the expenses involved in such a test would be quite high.

The equations of motion of the aircraft could be used to calculate the angle of attack and thus obtain the angle of downwash using this value of angle of attack and the measured angle of attack with the help of (9). But this method is not readily applicable for the T-28 as many modifications have been done to the aircraft for cloud penetration purposes, thus changing the constants involved in the aircraft's equation of motion.

To check the vertical velocity values computed by (16), a test flight should be conducted under conditions with no up- or downdrafts, in which the pilot induces some intentional pitching maneuvers. Then (16) can be used to calculate the vertical velocity; the result should be close to zero, and the departures would provide evidence of the accuracy of the equation.

## ACKNOWLEDGMENTS

First and foremost I would like to express my gratitude to Dr. P. L. Smith, Jr., for his guidance and help throughout this research. I thank Prof. W. N. Groves of the Mechanical Engineering Department for having allowed me to use the laboratory facilities of the Mechanical Engineering Department and for his assistance and also for his participation on my graduate committee. I also thank Dr. H. D. Orville and Mr. D. J. Musil for their help and cooperation as members of my graduate committee.

I take this opportunity to thank Dr. D. H. Lenschow of NCAR for sparing his time to review my thesis and giving suggestions for its improvement.

I thank Mr. J. L. Halvorson in running the computer programs and preparing the flight data for use in this research. I also thank Mr. J. R. Miller, Jr., Mr. G. N. Johnson, Mr. J. H. Killinger, Mr. J. E. Leigh, and Mr. J. Prodan for their assistance.

My special thanks to Mrs. C. H. Chen and Miss Carol Vande Bossche for their efforts in typing of the manuscript.

Also I thank all the other staff members and students of the Department of Meteorology for the encouragement they have given me during this research.

This research was performed as part of the National Hail Research Experiment, managed by the National Center for Atmospheric Research and sponsored by the Weather Modification Program, Research Applications Directorate, National Science Foundation, under Prime Contract No. NSF C-760, Subcontract No. NCAR 182-71.

## REFERENCES

- Auer, A., and W. R. Sand, 1966: Updraft measurements beneath the base of cumulus and cumulonimbus clouds. J. Appl. Meteor., 5, 461-466.
- Battan, L. J., 1973: Radar observations of the atmosphere. The University of Chicago Press, Chicago, 324 pp.
- Carlson, T. N., and R. C. Sheets, 1971: Comparison of draft scale vertical velocities computed from gust probe and conventional data collected by a DC-6 aircraft. NOAA Tech. Memo, ERL, NHRL-91, June 1971, 39 pp.
- Carter, C. C., 1929: Simple aerodynamics and the airplane. The Ronald Press Company, New York, 510 pp.
- Hurt, H. H., Jr., 1960: Aerodynamics for Naval aviators. NAVAIR 00-80T-80, U.S. Navy, 416 pp.
- Johnson, G. N., J. H. Killinger, D. J. Musil, and P. L. Smith, Jr., 1978: Cloud physics observations inside hailstorms with an armored aircraft data system. Preprints 4th Symposium on Meteor. Observations and Instrumentation, Amer. Meteor. Soc., 351-356.
- Kelly, T. J., and D. H. Lenschow, 1978: Thunderstorm updraft velocity measurements from aircraft. Preprints 4th Symposium on Meteor. Observations and Instrumentation, Amer. Meteor. Soc., 474-478.
- Lenschow, D. H., 1972: The measurement of air velocity and temperature using the NCAR Buffalo aircraft measuring system. NCAR Tech. Notes, June 1972.
- \_\_\_\_\_, 1976: Estimating updraft velocities from aircraft response. Mon. Wea. Rev., 104, 618-627.

Mason, B. J., 1962: Clouds, Rain, and Rainmaking. Cambridge University Press, Cambridge, 189 pp.

Rockwell International, 1955: Revised performance data for Navy Model T-28B Trainer. Report No. NA-55H-365, North American Aviation, Inc.

Sand, W. R., 1974: Use of the armored T-28 aircraft to obtain observations in hailstorms with emphasis on the characteristics of the high radar reflectivity zones. Report 74-14, Institute of Atmospheric Sciences, South Dakota School of Mines and Technology, Rapid City, South Dakota, 76 pp.

Shapiro, A. H., 1953: The dynamics and thermodynamics of compressible fluid flow. The Ronald Press Company, New York, 647 pp.

## APPENDIX A

## Zero Setting of Pitch Angle Indicator

It was observed that the gyro governing the pitch indicator was not aligned with the vertical axis of the T-28. But it was oriented in a plane perpendicular to the lateral axis of the aircraft. This resulted in the pitch reading to be offset by a few degrees. The correction thus required was estimated as follows from a tower fly-by data. It is evident from Fig. 2 that if there were no vertical air motions the pitch and the angle of attack should be equal in level flight. So a sample of data points was selected from the tower fly-by data when the aircraft is in level flight. Then the mean pitch angle and the mean angle of attack were found. It was seen that the indicated pitch angle was  $2.25^\circ$  in excess. So

$$\text{Pitch angle} = \text{Indicated pitch angle} - 2.25^\circ$$

The data used to calculate this is given in Table 3.

TABLE 3

Pitch and Angle of Attack in Level Flight  
Free of Vertical Air Motions

<u>Angle of Attack Digital Count</u>	<u>Angle of Pitch in Degrees</u>
480	7
476	7
477	6
480	6
480	6
490	7
511	10
508	9
481	8
470	7
465	7
478	7
479	6
486	6
493	7
491	7
488	7
483	6
489	7
Mean	7.15
485.65	

Measured angle of attack in degrees = (Digital count - 441) 0.0526

Mean measured angle of attack = 2.35°

From (11)

Mean angle of attack = 4.9°

In level flight with no vertical air motions

Angle of pitch = Angle of attack

Zero correction to the pitch angle = Mean angle of attack - mean

pitch = -2.25°